DILATANCY OF QUARTZ GOUGE IN PURE SHEAR

Barry Raleigh and Chris Marone

Lamont-Doherty Geological Observatory of Columbia University
Palisades, New York

Abstract. Dilatancy in artificial fault gouge consisting of quartz sand is produced under pure shear loading conditions at shear stresses of about 1/2 the frictional shear failure strength. The gouge, in a layer at 45° to the axis of a confined cylindrical sample, is maintained at constant normal stress and internal pore pressure while increasing the shear stress. Repeated cycles to failure result in compaction of the gouge up to shear strains of about 0.3 and porosity of about 15%, after which the gouge shows porosity increases upon shear and decreases upon unloading. The rate of change of porosity with shear stress, $d\phi/d\tau$, is about $2 \times 10^{-4} MPa^{-1}$, at about 45 to 100 MPa effective normal stress, increasing at lower normal stress.

The shear stress at the onset of dilatancy, is nearly independent of normal stress and confining pressure and is considerably lower than has been previously observed. Pure shear loading may be nearer to the conditions for natural loading of strike slip or normal faults than triaxial loading, and we conclude that dilatancy should occur prior to earthquakes in natural fault zones.

Introduction

Understanding the processes responsible for the destabilization of faults and the ensuing earthquakes probably contains the key to predicting earthquakes. Some of the early optimism that earthquakes should be predictable arose from laboratory observations of markedly non-linear stress-strain behavior in rocks just prior to shear failure. F. C. Frank (1965) proposed that one of the mechanical processes known to precede shear failure, namely dilatancy, should lead to instability. Brace and his co-workers (Brace, et al., 1966; Schock, et al., 1973; Hadley, 1973; Jones, 1980; Scholz and Kranz, 1974) and others (Edmonds and Paterson, 1972; Zoback and Byerlee, 1975; Weeks, 1980; Teufel, 1981) examined dilatant volume changes in rock and gouge under various confining pressures and differential stresses. Brace, et al. (1966) found that at differential stresses about half the fracture strength of confined, intact Westerly granite, volumetric strains departed from linear, increasingly negative dilation to positive dilation with increases of axial stress and constant confining pressure. They attributed the volume increase to the opening of microcracks within the granite cylinder.

In loosely compacted soils or sands, dilatancy has long been known to occur (Youd, 1972) although only after considerable compaction of the original pore space takes place during the initial increments of inelastic strain. Intact specimens of marble, limestone, sandstone and talc subjected to 20% axial strain, even though macroscopically ductile, show net dilatant volumetric strains following initial compaction when the confining pressures are less than 200 to 400 MPa (Edmonds and Paterson, 1971). At higher confining pressures (400 to 800 MPa) the plasticity of calcite and talc suppresses dilatant cracking but the sandstone becomes dilatant after about 10% longitudinal strain. Thus, even in the ductile regime, microcracking may occur in intact rock at sufficiently high shear stresses or shear strains, although the phenomenon is more pronounced at lower confining pressures.

Dilatancy was seized upon by Nur (1972) and Scholz, et al. (1973) as a means for explaining apparently anomalous negative excursions in the ratio of shear to compressional wave travel times in the region surrounding impending earthquakes in Central Asia (Nersesov, et al., 1971), and the timing of precursory phenomena relative to the magnitude of the earthquakes. Pointing out that undersaturated rocks have a Vp/Vs ratio about 5% less than saturated ones, Nur proposed that dilatancy, causing undersaturation followed by diffusion of pore water into the pore space to resaturate the rocks, would lead to the observed velocity anomalies. However, with few exceptions (Aggarwal, et al., 1973) subsequent observations have failed to establish the Vp/Vs anomaly as a phenomenon precursory to earthquakes elsewhere.

Hadley (1973) noted that, experimentally, dilatancy was not observed in intact rocks until the stresses on the potential failure surface exceeded the frictional strength for sliding on pre-existing cracks. Therefore, Hadley reasoned that frictional failure on faults would occur before

Copyright American Geophysical Union

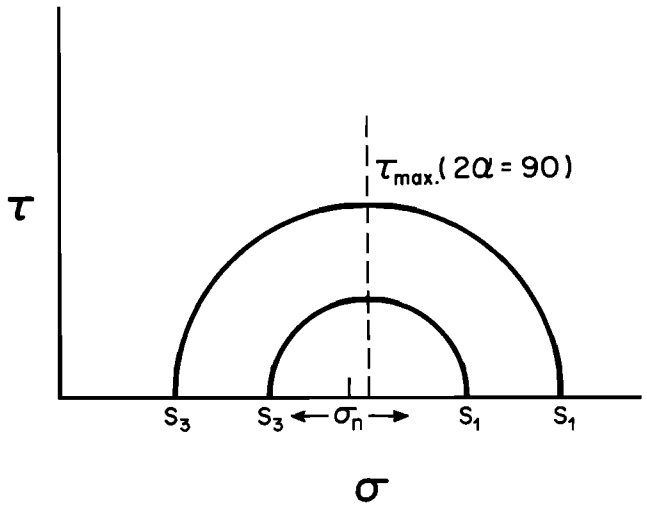

Fig. 1. Mohr diagram showing shear stress, τ_{max}, and effective normal stress, σ_n, for maximum, S_1, and least, S_3, total principal compressive stresses in the pure shear loading conditions of these experiments. The arrows indicate paths of S_1, and S_3 upon increasing shear stress. Normal, σ_n, and mean stress on 45° gouge layer are constant.

any appreciable dilatant volume change could take place. If correct, Hadley's (1973) evidence would explain the paucity of velocity anomalies prior to large earthquakes and dilatancy-diffusion would not be an interesting candidate for the explanation of other precursory anomalies.

Zoback and Byerlee (1976), Weeks and Byerlee (1978) and Jones (1980) showed that loading history plays a role in the onset of dilatancy. If a sawcut or crushed sample is taken repeatedly through the loading-to-failure-unloading cycle, dilatant behavior accompanies the onset of frictional sliding. Their conclusions are similar to Hadley's, namely that dilatancy occurs only at or above stresses required for frictional sliding. Moreover, Teufel (1981) notes that dilatancy accompanies frictional sliding on pre-cut surfaces and is restricted to a narrow region immediately adjacent to the sliding surfaces. He concludes that such changes in physical properties that might accompany dilatancy in natural fault zones would conceivably be too localized for measurement of precursory changes. However, Holcomb (1978), through measurement of compressional wave velocities in triaxially loaded Westerly granite, showed that the onset of dilatancy occurs at $\tau/\sigma_n = 0.47$, a ratio which is somewhat less than the measurements of sliding frictional strength of saturated Westerly granite gouge (Vaughan and Byerlee, 1985) of $\tau/\sigma_n = 0.65$.

All the experiments cited above were performed under triaxial loading, in which axial stress is increased while the two other principal stresses are held constant and equal to the confining pressure. Thus, it is difficult to deduce from the experimental data how dilatant volume changes with different general states of stress. In triaxial loading, the shear, normal and mean stresses all increase in a dilatant zone along a suitably inclined fault or gouge layer. Pore volume increases due to increased shear stress would encounter the competing effect of increased mean stress.

The variation in state of stress with time on natural faults is not known. In reverse faults, in which S_3, the overburden pressure, remains constant, increasing S_1 to failure means that the normal stress must increase along with the shear stress. Ideally, strike-slip faults are driven to failure by pure shear loading, i.e., $\Delta S_1 = -\Delta S_3$. However, the only data, derived from geodetic strain measurements (Raleigh, et al., 1982) indicate that the normal stress on strike-slip faults may increase along with shear stress. Finally, normal faults should experience decreasing normal stress during loading, inasmuch as S_1, the overburden pressure remains constant. In the normal and strike-slip cases, pure shear loading should more closely approximate the natural conditions than conventional triaxial loading.

The experiments described below were performed on a layer of simulated gouge of Ottawa sand under conditions of loading which allow changes of shear stress but maintain constant the normal and mean stress on the gouge layer. The stress state is that of pure shear, $\Delta\sigma_{11} = -\Delta\sigma_{33}$, one which is generally assumed to approximate the loading conditions for strike-slip faulting. The Mohr diagram in Figure 1 illustrates the maximum shear stress and normal stress across the gouge layer in relation to the axial stress S_1, and the confining pressure, S_3.

Experimental Procedure

We prepared ~3-5 mm thick layers of fine (0.5-0.8 mm) Ottawa quartz sand between serrated surfaces of a steel cylinder cut at 45° to the cylinder axis (Figure 2). The jacketed cylinder was confined by fluid pressure at room temperature in a triaxial loading apparatus (Scholz and Koczynski, 1979). An internal load cell provided the input to a servo-controller which reduced the confining pressure by the amount of increase in the axial stress. Details of the experimental set-up are given in Marone and Raleigh (in prep.).

The dilatant volume changes were monitored by metering the volume of water required to maintain the pore pressure constant within the gouge layer. The technique is used commonly and provides accuracy in pore volume strain in our experiments of $\pm 10^{-6}$. The permeability of the gouge throughout the experiments remained high enough so that the internal pore pressure equilibrated to 90% of its final value within less than 10 seconds following application of a pressure transient.

The shear stress, τ, was derived from measurements of axial load using an internal load cell and was just equal to the axial stress less the

Copyright American Geophysical Union

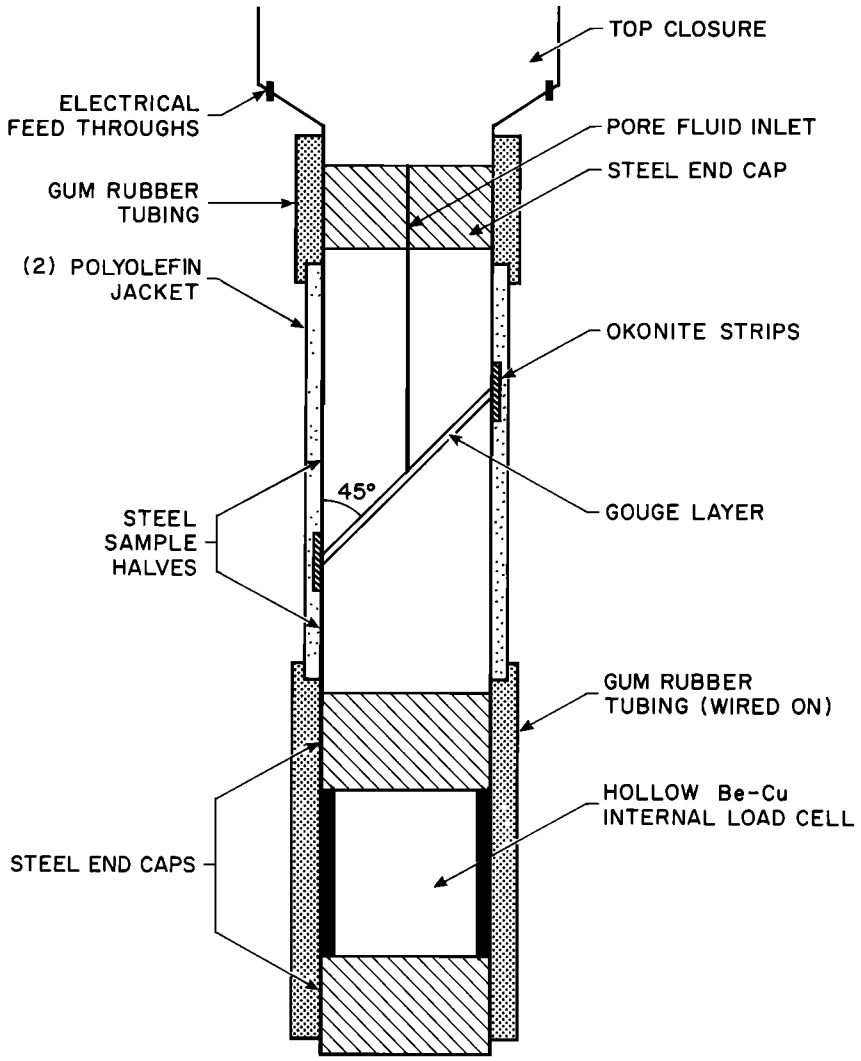

Fig. 2. Cross section of sample assembly for gouge deformation experiments.

initial confining pressure at the onset of loading. The normal stress, σ_n, was equal to the initial confining pressure less the internal pore pressure (Figure 1) and remained constant unless purposely reset to another confining pressure.

We initially pre-compacted the gouge under hydrostatic pressure of 100 MPa to a porosity of about 20%. The confining pressure was then set at some value in the range 30 to 100 MPa and axial load increased by advancing the piston at a constant displacement rate, normally 1 μm sec^{-1}. As noted above the confining pressure was decreased to maintain the normal stress constant. In most experiments, axial stress was cycled repeatedly. After some inelastic deformation was recorded, then axial stress was reduced to half or less of the stable-sliding shear stress and then increased again to the stable-sliding regime. During each cycle, the normal stress remained constant through the method described above.

Experimental Results

In Figure 3, shear stress and porosity are plotted against shear strain in a typical experiment. The gouge compacts from its initial porosity of ∿20% to a porosity of approximately 10 to 15% after an inelastic shear strain of about γ=0.3. There is a reduction in average grain size to 10 to 30 μm accompanying the porosity reduction. At higher shear strains, the gouge porosity remains approximately constant, the volume increase upon shearing being about equivalent to the decrease upon relaxation of shear stress through

Copyright American Geophysical Union

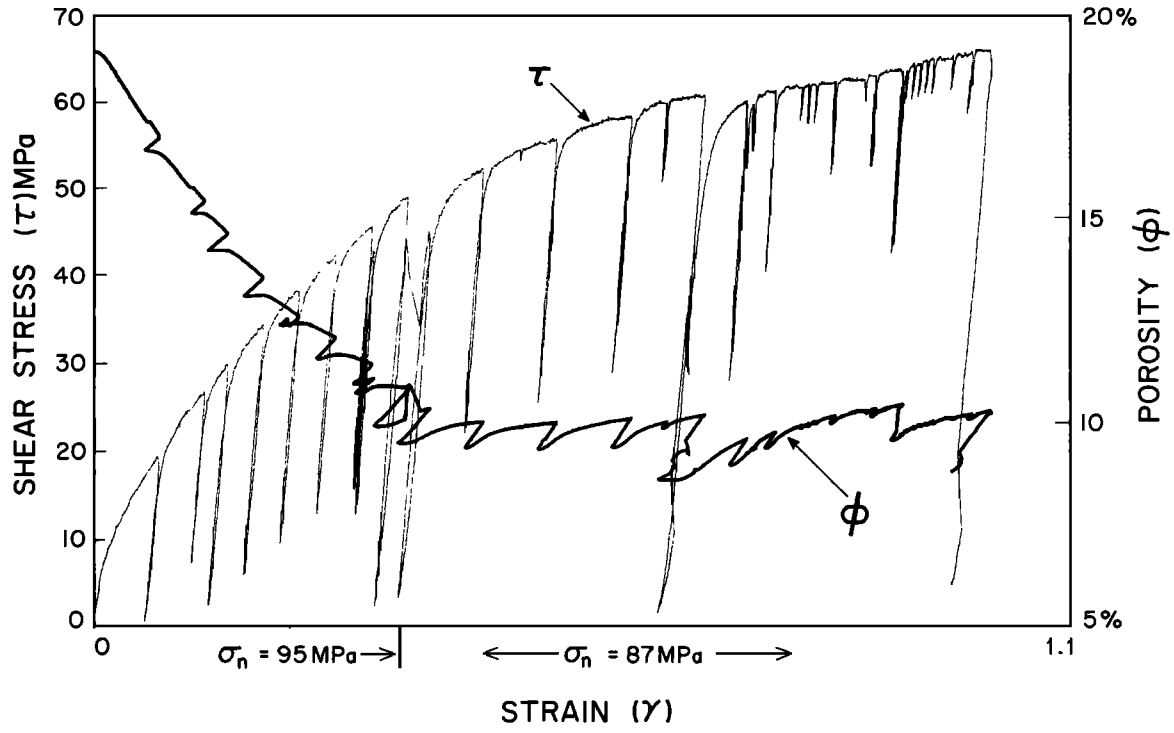

Fig. 3. Stress-strain curve for quartz gouge deformed in cyclical, pure shear loading. Porosity is ϕ, σ_n is effective normal stress on 45° gouge layer, τ is shear stress, γ is shear strain. (Exp. 16)

the repeated cycles of loading and unloading. In one experiment performed without cycling, we observed no dilatant volume increase and the porosity vs shear strain curve was similar to that of Figure 3 without the excursions due to cycling.

The results shown in Figure 3 are similar to our other experiments at different values of σ_n in several respects. From the outset of loading, a small linear increase of shear stress with shear strain gives way to a period of non-linear and strongly work-hardening stress-strain behavior during the phase of rapid compaction of the gouge. At the strain level where the net compaction has disappeared (Figure 3), the slope of the stress-strain curve decreases to a slowly work-hardening phase which we take to be associated with a nearly constant net pore volume in the gouge. This steady-state average porosity is about 15% ±5% independent of confining pressure. The ratio of τ_s/σ_n in the steady-state regime varies between 0.5 and 0.8 with a mean value of μ=0.65.

Upon cycling, the stress-strain behavior is nearly linear except at low shear stresses and at those within about 95% of the stress for stable-sliding. The pore volume during loading in the steady state region (Figure 4) begins to increase linearly at a shear stress, τ_D, which is about half the shear stress required for stable sliding, τ_s. The ratio, τ_D/τ_s, ranges from about 0.3 to 0.7. Where stable sliding occurs, the pore volume continues to increase but at a lower slope with strain than in the elastic part of loading curve before failure (Figure 4). Upon unloading, the pore volume decreases along a linear path down to about $0.1\tau_s$, where the slope decreases. The slope of the curve of volume decrease upon reduction in shear stress is consistently greater than the slope on increase of shear stress.

Discussion of Experimental Data

The Onset of Dilatancy

For each experiment, we analyse the data for the following parameters as illustrated in Figure 4. The value of τ_D is the shear stress at the onset of dilatancy; τ_s is the shear stress for stable-sliding and $\Delta\tau_E$ is the approximately linear change in shear stress with strain during loading or unloading accompanied by positive or negative dilatant volume changes. The dilatant porosity change associated with $\Delta\tau_E$ is $\Delta\phi_E$ (Figure 4).

The onset of dilatancy, shown in Table 1 as τ_D and in the ratio τ_D/τ_s, varies from about 10 to 25 MPa in those cycles starting from near-zero shear stress. There is apparently not a strong dependence on normal stress or loading rate, $\dot{\delta}$, at least within the range σ_n=30 to 100 MPa and $\dot{\delta}$=1 to 6 μms^{-1}. As noted previously, τ_D/τ_s decreases from about 2/3 at σ_n = 30 MPa to 1/3 at σ_n = 100

Copyright American Geophysical Union

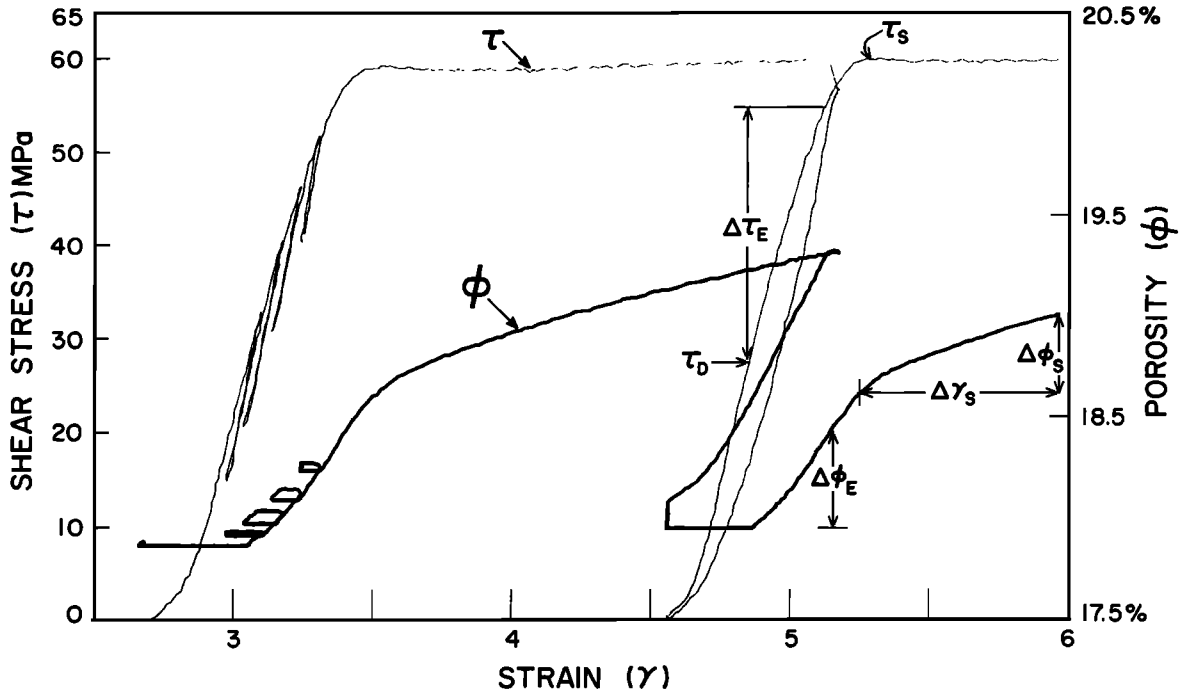

Fig. 4. Stress-strain-porosity relation through a complete cycle, τ_n is shear stress at onset of dilatancy, $\Delta\tau_E$ is approximately linear increase of shear stress from τ_D to failure and $\Delta\phi_E$ is change in porosity over $\Delta\tau_E$. γ_s is inelastic shear strain and $\Delta\phi_s$ is the associated porosity change.

MPa. This result compares with $\tau_D/\tau_s \approx 1$ in standard triaxial experiments on fault gouge or crushed rock (Zoback and Byerlee, 1975; Jones, 1980).

Because of the special loading conditions of these experiments, the magnitude of the effective principal stresses, σ_1, and σ_3, at the onset of dilatancy are just given by, from Figure 1,

$$\sigma_1 = \sigma_n + \tau_D \quad (1)$$

$$\sigma_3 = \sigma_n - \tau_D \quad (2)$$

From Table 1, and (1) and (2), the graph in Figure 5 of σ_1 vs σ_3 at the onset of dilatancy is derived. The values of σ_n are shown on the graph. Thus, for cycles in which τ_n is increased from near-zero and loading rates are less than 10 μs^{-1}, dilatancy in our samples is initiated at principal effective stresses

$$\sigma_1 = 26 + 1.2\sigma_3 \quad \text{(MPa)} \quad (3)$$

and the dependence of τ_D on confining pressure (at $80>\sigma_3>10$ MPa and $128>\sigma_1>40$ MPa) is given by

$$\tau_D = 13 + 0.1\sigma_3 \quad \text{(MPa)} \quad (4)$$

The result above may not be of very general applicability inasmuch as loading in pure shear is a special case in nature as is pure quartz sand with porosity of 10 to 20%. Moreover, we have not investigated the effect of time on the properties of gouge or of confining pressure less than about 10 MPa. Presumably, some degree of healing of cracks and welding of grain boundaries would come about if long rest times between loading cycles were employed. Also, if the stress drop in earthquakes were a small fraction of the failure stress the inception of increase of dilatancy would begin at or above the minimum shear stress and the relationships (3) and (4) would not apply. Nevertheless, we may draw the important conclusion that the onset of dilatancy in this granular material, upon cycling of the shear stress in pure shear, occurs at about half the frictional sliding stress and is independent of the effective confining pressure for values of σ_3 likely to be encountered in the brittle crust.

Variation in Dilatant Porosity with Shear Stress

The observations discussed here are derived from the approximately linear increases and decreases in pore volume, $\pm\Delta V_E$, measured in the steady-state region upon loading near failure and unloading following frictional sliding. We compute the change in porosity, $\Delta\phi_E$, from $\frac{\Delta V_E}{V_o}$, where V_o is the gouge volume following the initial stage of compaction (Figure 3). The change in porosity, $\Delta\phi_E$ is divided by $\pm\Delta\tau_E$, the approximately linear

Copyright American Geophysical Union

TABLE 1. Shear Stresses τ_D at Onset of Dilatancy, and τ_s, at Frictional Sliding; μ, the Coefficient of Sliding Friction; σ_n is the Effective Normal Stress and σ_{3D}, the Effective Least Principal Stress at the Onset of Dilatancy

Experiment	τ_D MPa	τ_s MPa	τ_D/τ_s	σ_n MPa	τ_s/σ_n (μ)	σ_{3D} ($\sigma_n-\tau_D$)MPa
37	15.5	24.9	0.62	30.5	0.81	15.0
40	14.2	22.7	0.63	30	0.76	15.8
	15.8	22.7	0.70	30	0.76	14.2
	15.9	22.7	0.69	30	0.77	14.1
	28.0	47.0	0.60	72	0.65	44.0
24	17.9	23.5	0.76	45.7	0.52	27.8
	10.0	25.0	0.40	45.7	0.55	35.7
	12.2	26.8	0.46	45.7	0.59	35.3
	13.8	28.3	0.49	45.7	0.63	33.7
20	19.2	35.5	0.54	60	0.59	40.8
	21.2	37.0	0.57	60	0.62	38.8
	21.2	37.1	0.57	60	0.62	38.8
	23.2	37.4	0.62	60	0.62	37.8
	21.9	38.1	0.57	60	0.64	38.1
	20.3	38.4	0.53	60	0.65	39.7
	11.6	37.3	0.31	60	0.62	48.4
26	14.4	43.7	0.33	66	0.66	51.6
	16.8	44.6	0.38	66	0.67	49.2
	14.9	47.5	0.32	66	0.72	51.1
	18.2	49.4	0.37	66	0.75	47.8
	17.3	51.8	0.33	66	0.78	48.7
44	16.8	34.4	0.49	65	0.53	48.2
16	20.8	55.5	0.37	86.7	0.64	65.9
	19.8	53.5	0.37	86.7	0.62	66.9
	18.3	47.0	0.39	93.0	0.51	74.7
38	20.5	55.0	0.37	101	0.54	80.5
	25.6	54.9	0.47	101	0.54	75.4

increase or decrease of stress on loading or unloading (Figure 4) to give $d\phi_E/d\tau_E$. The shear strains, γ_E, over which $\Delta\tau_E$ and $\Delta\phi_E$ are measured are given in Table 2 along with the normal stress, σ_n, for each cycle. The data in Table 2 give a few cycles for each of the experiments but the complete results are shown in Figure 6, a plot of $d\phi_E/d\tau_E$ against σ_n.

In Figure 6, $d\phi_E/d\tau_E$ varies from about 0.5 to 10 x 10^{-4}MPa^{-1}. The decrease in porosity upon unloading is about twice the increase upon loading in successive cycles at the same normal stress. At any given normal stress, especially below about 70 MPa, $d\phi_E/d\tau_E$ varies by about a factor of two in either the loading or unloading cycles.

There is a pronounced effect of normal stress on the magnitude of $d\phi_E/d\tau_E$ measured on the unloading cycle as shown in Figure 6. With a large scatter, $d\phi_E/d\tau_E$ on unloading varies from 8 x 10^{-4}MPa^{-1} at 30 to 45 MPa normal stress to about 1.8 x 10^{-4}MPa^{-1} at 93 to 100 MPa normal stress. On both loading and unloading, the variability in $d\phi_E/d\tau_E$, is reduced at the higher normal stress.

Values of $d\phi_E/d\tau_E$ on loading lie between 0.6 and 2.5 x 10^{-4}MPa^{-1} for all normal stresses above 30 MPa, where the average value is 5 x 10^{-4}MPa^{-1}. At 30 MPa normal stress, at τ_D, the ratio of the maximum to least effective principal stresses is about $\frac{\sigma_1}{\sigma_3}\simeq 3$ with σ_3 dropping from about 15 to 5 MPa as $\tau \to \tau_s$. The local tensile stresses which must occur at such low confining pressures probably account for the large and erratic values of change in porosity.

From Figures 3 and 4, porosity also increases during stable sliding in the gouge. The effect is observed either with or without work-hardening.

Copyright American Geophysical Union

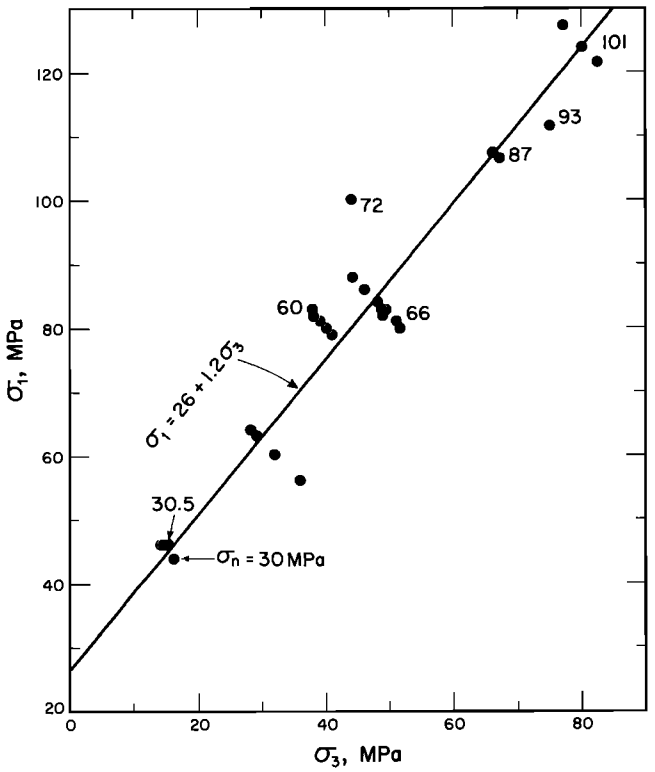

Fig. 5. σ_1 and σ_3 at onset of dilatancy at different normal stresses, σ_n.

The rate of increase of porosity declines with increasing amounts of sliding as Figures 3 and 4 suggest. We observe the ratio $d\phi_s/d\gamma_s$ to lie between about 0.02 and 0.1. Thus, a shear strain of 1 might result in an increase in porosity of 2% to 10% at nearly constant shear stress.

During sudden stress drops in the occasional stick-slip events encountered, the net porosity change is negative and comparable in magnitude to those measured upon deliberate unloading, i.e., about 2 x 10^{-4}MPa^{-1} to 9 x 10^{-4}MPa^{-1}. The strains were positive in stick-slip rather than negative; however, being small events of stress drop no more than 2 to 10 MPa, displacements were correspondingly small, about 1 to 4 μm.

Discussion and Conclusions

Summary

To summarize our findings briefly, we note:

1) Under conditions of pure shear loading, where σ_n is held constant and the shear stress, τ, is increased, fault gouge consisting of quartz sand first compacts to a steady-state porosity of 15 ± 5%. Cyclical loading producing 5 to 20% permanent shear strain in each cycle causes dilatant porosity changes.

2) The onset of dilatancy occurs at shear stresses, τ_D, about 1/3 to 2/3 of the shear stress required for stable sliding. There is a slight positive effect of σ_3 on τ_D, which, for normal stresses between 30 and 100 MPa, has a mean value of 19 MPa. The coefficient of sliding friction calculated for a 45° sliding surface (Table 2) has a mean value of $\mu = 0.64$.

3) The dilatant porosity changes are positive on loading and negative upon unloading. From the onset of dilatancy with rising shear stress to near the point of failure, the porosity changes linearly by, approximately,

$$d\phi_E/d\tau_E = 1.5 \times 10^{-4}\text{MPa}^{-1}$$

at normal stresses greater than about 40 MPa.

The porosity decrease, $d\phi_E/d\tau_E$, upon unloading is about twice that for loading, as much as 6 to 9 x 10^{-4}MPa^{-1} at normal stresses below 46 MPa. Increased normal stress results in smaller values, about 2 x 10^{-4}MPa^{-1}.

Inelastic shear strain also causes increased dilatant volume as noted widely by others (Jones, 1980; Zoback and Byerlee, 1975). For a shear strain of 1, the porosity should increase by less than 10%.

Mechanism of Dilatancy

Dilatancy in intact rocks is related to the opening of microfractures upon increase in differential stress (Brace, et al., 1966). Our data contribute little to discussions on the mechanism of dilatancy in gouge although it appears that both the onset of dilatancy and the change in porosity vs shear stress, $d\phi_E/d\tau_E$, are only weakly dependent on normal stress or on σ_3, the least principal compressive stress. If opening of microfractures oriented either randomly or parallel to σ_1, give rise to dilatancy, then normal stress (= mean stress) or σ_3 should have a more pronounced effect on τ_D or on $d\phi_E/d\tau_E$. Only at low values of σ_3 of 5 to 15 MPa is the effect of confining pressure important to $d\phi_E/d\tau_E$.

More favorably oriented microcracks, e.g., at 30° to σ_1, might slip before macroscopic frictional failure on the 45° gouge layer occurs. Sliding on microcracks would open new pore volume at triple junctions of cracks or at bends. Furthermore, the hysteresis in stress-strain behavior upon cycling requires work to be done which could be readily explained by frictional sliding on microcracks (Walsh, 1965; Scholz and Kranz, 1974; Holcomb, 1978).

Although we have not examined the geometry of microcracks in the deformed gouge, we assume there to be adequate numbers of favorably oriented cracks and grain boundaries in the crushed, granular quartz gouge after compaction and cycling. If one further assumes that the internal stresses are the same as the applied stress, the condition for frictional sliding at the onset of dilatancy on the favorably oriented cracks is

Copyright American Geophysical Union

TABLE 2. Variation in Porosity with Shear, τ_E, and Normal, σ_n, Stress

Experiment	ΔV_E (cm^3)	$\frac{\Delta V_E}{V_o}$ ($\Delta\phi_E \times 10^{-3}$)	$\Delta\tau_E$ (MPa)	$d\phi_E/d\tau_E$ ($\times 10^{-4}$)	σ_n (MPa)	$\Delta\gamma$	$G\Delta\tau_E/\Delta\gamma$ MPa
33	0.014	3.5	9.0	3.9	30	0.052	170
	-0.058	-14.5	-20.8	7.0	30	-0.076	270
	0.014	3.5	5.8	6.0	30	0.040	140
	0.019	4.8	9.5	5.0	30	0.040	240
	-0.053	-13.3	-15.7	8.5	30	-0.028	560
24	0.008	2.1	21.7	1.0	46	0.068	320
	-0.048	-13.4	-21.7	6.1	46	-0.044	490
	0.016	4.6	22.0	2.1	46	0.068	320
	-0.077	- 9.5	-22.5	4.2	46	-0.044	510
20	0.008	1.8	12.0	1.5	60	0.028	430
	-0.038	- 8.1	-31.1	2.6	60	-0.068	460
	0.012	2.6	12.5	2.1	60	0.032	390
	-0.040	- 8.6	-31.8	2.7	60	-0.078	410
	0.011	2.4	12.8	1.9	60	0.024	530
26	-0.082	-19.9	-39.8	5.0	66	-0.068	580
	0.029	7.0	24.9	2.8	66	0.040	620
	0.024	5.8	23.5	2.5	66	0.040	590
	-0.027	- 6.6	-18.2	3.6	66	-0.018	1000
	0.017	4.1	13.4	3.1	66	0.024	560
	-0.042	-10.2	-24.0	4.2	66	-0.028	860
	0.015	3.6	16.8	2.1	66	0.024	700
16	-0.054	- 9.6	-40.1	2.4	87	-0.036	1110
	0.018	3.3	32.7	1.0	87	0.032	1020
	-0.041	- 7.3	-28.7	2.5	87	-0.020	1430
	0.021	3.7	23.8	1.5	87	0.025	950
	-0.045	- 7.9	-28.2	2.8	87	-0.022	1280
	0.019	3.4	24.6	1.3	87	0.025	980
	0.008	1.3	23.7	0.6	93	0.019	1250
	-0.032	- 5.7	29.2	1.8	93	-0.022	1330
	0.010	1.9	21.8	0.8	93	0.021	1040
	-0.024	- 4.3	28.8	1.7	93	-0.022	1310
	0.012	2.1	25.7	0.8	93	0.022	1170

$$\frac{\tau_D}{\sigma_n} \geq \frac{\sqrt{3}(\sigma_1-\sigma_3)}{\sigma_1 + \sigma_3} \qquad (5)$$

assuming μ to be 0.566. The condition in (5) is satisfied, using relations (1) and (2) and taking $\mu = 0.566$, only at $\sigma_n \leq 30$ MPa. At higher normal stresses τ_D/σ_n is around 0.3 on 30° microcracks, about half the sliding friction. Reverse sliding on microcracks during unloading is not an attractive mechanism for dilatant closure of porosity. As Holcomb (1978) notes, closure of porosity should only occur after a drop in the shear stress and we find that the porosity decrease is linear with decreasing shear stress with no lag.

Dilatancy and Earthquakes

Dilatancy and fluid diffusion may be important in the failure process in earthquakes if dilatant volume changes are appreciable prior to the earthquakes. If, as the Rangely experiment showed (Raleigh, et al., 1976), earthquake failure is initiated when stresses exceed the sliding frictional strength, then dilatancy must occur before those stresses are reached. Our data indicate that, at least for pure shear loading conditions, dilatancy may be initiated at stresses well below those required for rupture.

Indeed, provided crushed quartz sand is not too unlike the gouge in large strike slip faults, dilatancy may precede earthquakes for a substantial fraction of the earthquake cycle time. The problem with detecting dilatancy-induced precursory effects may thus ultimately reside in their longevity, particularly if the pore volume increases linearly with shear stress. If dilatancy

Copyright American Geophysical Union

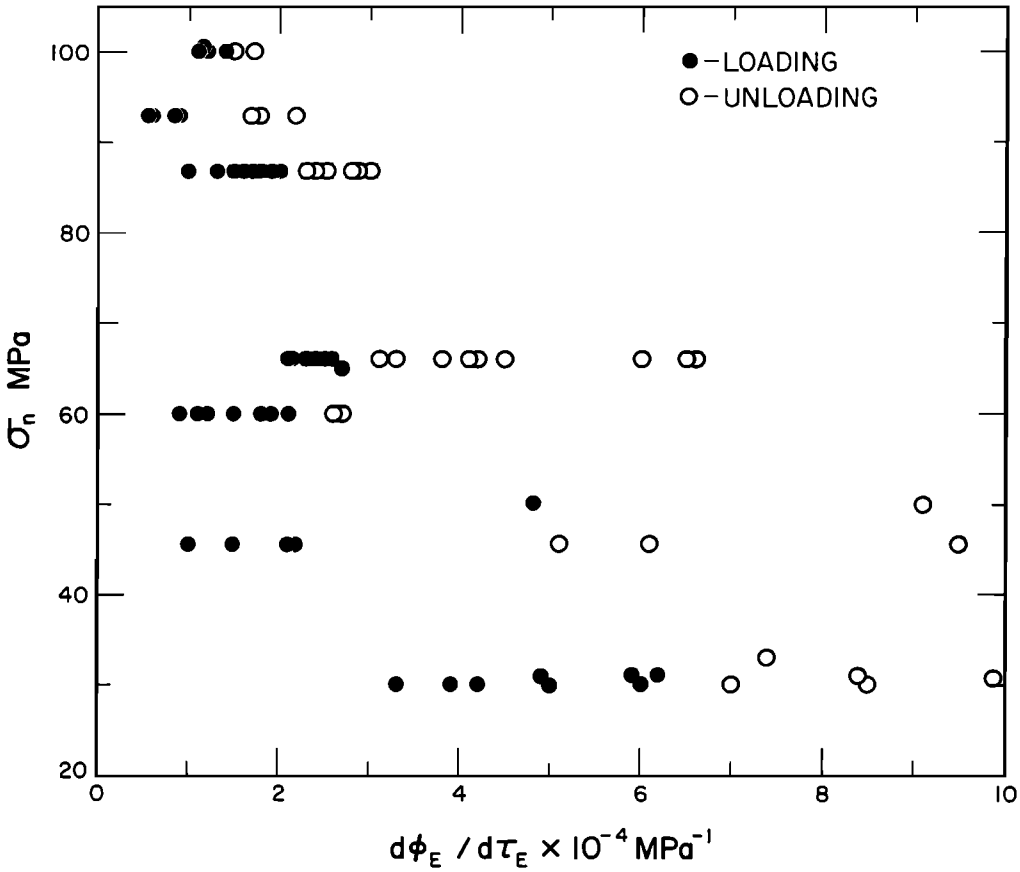

Fig. 6. Change in porosity with shear stress vs normal stress, σ_n.

is not a short-lived, non-linear phenomenon, it may not prove to be useful for earthquake prediction. However, the effects of differing gouge materials, temperature and time remain to be explored.

We have artifically constrained dilatancy to the gouge layer by employing steel cylinders instead of rock. However, variations in fluid diffusivity, seismic velocity and possible sudden pore pressure increases upon collapse of dilatant volume during sudden stress drops, will also depend on the dilatancy-induced porosity in the rocks bordering a fault. Future experiments using pure shear or triaxial extension need to be conducted to determine whether dilatancy precedes frictional sliding stresses in intact rock as well as in gouge.

Acknowledgements. Critical comments provided by C. Scholz and T. N. Narasimhan were most helpful. Ted Koczynski provided invaluable aid in preparing the experimental apparatus. This research was supported through U.S.G.S. contract 14-08-0001-G-952.

References

Aggarwal, Y. P., L. R. Sykes, J. Armbruster, and M. L. Sbar, Premonitory changes in seismic velocity and earthquake prediction, Nature, 24, 101, 1973.

Brace, W. F., B. W. Paulding, Jr., and C. H. Scholz, Dilatancy in the fracture of crystalline rock, J. Geophys. Res., 71, 3939-3953, 1966.

Edmonds, J. M., and M. S. Paterson, Volume changes during the deformation of rocks at high pressures, Int. J. Rock Mech. Min. Sci., 9, 161-182, 1972.

Frank, F. C., On dilatancy in relation to seismic source, Rev. Geophys. Space Phys., 3, 485-503, 1965.

Hadley, K., Laboratory investigation of dilatancy and motion on fault surfaces at low confining pressures, Proc. Conf. Tect. Prob. San Andreas Fault Zone, edited by Kovach R. L. and Nur A., Stanford Univ. Publ. Geol. Sci., 13, 427-435, 1973.

Holcomb, D. J., A quantitative model of dilatancy in dry rock and its application to Westerly granite, J. Geophys. Res., 83, 4941-4950, 1978.

Jones, L. M., Cyclic loading of simulated fault gouge to large strains, J. Geophys. Res., 85, 1826-1932, 1980.

Nersesov, I. L., A. N. Semenov, and I. G. Simbireva, Space time variations of t_s/t_p in

Copyright American Geophysical Union

Garm, Experimental Seismology, v334, (in Russian) 1971.
Nur, A., Dilatancy, pore fluids, and premonitory variations of t_s/t_p travel times, Bull. Seismol. Soc. Amer., 62(5), 1217-1222, 1972.
Nur, A., A note on the constitutive law for dilatancy, Geofis. Pura Appli., 113, 69-86, 1975.
Raleigh, C. B., J. H. Healy, and J. D. Bredehoeft, An experiment in earthquake control at Rangely, CO, Science, 191, 1230-1237, 1976.
Raleigh, C. B., D. L. Anderson, K. Sieh, and L. R. Sykes, Forecasting southern California earthquakes, Science, 217(4565), 1097-1104, 1982.
Rowe, P. W., The stress-dilatancy relation for static equilibrium of an assembly of particles in contact, Proc. Roy. Soc., Ser. A., 269(1339), 500-527, 1962.
Schock, R. N., H. C. Heard, and D. R. Stephens, Stress-Strain Behavior of a Granodiorite and Two Graywackes on Compression to 20 Kilobars, J. Geophys. Res., 78, 26, 5922-5941, 1973.
Scholz, C. H., and T. A. Koczynski, Dilatancy anisotropy and the response of rock to large cyclic loads, J. Geophys. Res., 84, 5525-5534, 1979.
Scholz, C. H., and R. Kranz, Notes on dilatancy recovery, J. Geophys. Res., 79, 2132-2135, 1974.
Scholz, C. H., L. R. Sykes, and Y. P. Aggarwal, Earthquake prediction: A physical basis, Science, 181, 803-810, 1973.
Teufel, L. W., Pore volume changes during frictional sliding of simulated faults, Geophys. Monograph 24, Mechanical behavior of crustal rocks, 135-145, 1981.
Vaughan, P., and J. Byerlee, Frictional sliding in saturated westerly granite: effect of slip rate, The Fifth Ewing Symp. on Earthquake Source Mechanics, v6, eds. S. Das, J. Boatwright, and C. Scholz, AGU Monograph, Washington, D.C., in press, 1985.
Walsh, J. B., The effect of cracks on the uniaxial elastic compression of rocks, J. Geophys. Res., 70, 399-411, 1965.
Weeks, J., Some aspects of frictional sliding at high normal stress, Ph.D. Thesis, Stanford University, Stanford, CA, 171 pp., 1980.
Weeks, J., and J. Byerlee, Preliminary investigation of volume changes in crushed granite preceding stick-slip failure, Geophys. Res. Letters, 5, 832-834, 1978.
Youd, T. L., Compaction of sands by repeated shear straining, J. of Soil Mechanics and Foundations Divisions, Proc. of the American Soc. of Civ. Eng., 98, 709-725, 1972.
Zoback, M. D., and J. D. Byerlee, The effect of cyclic differential stress on dilatancy in Westerly granite under uniaxial and triaxial conditions, J. Geophys. Res., 80, 1526-1530,1975.

Copyright American Geophysical Union